


A refined disturbance rejection control for vibration suppression of smart structures under unknown disturbances

Journal of Low Frequency Noise,
Vibration and Active Control
0(0) 1–15
© The Author(s) 2019
DOI: 10.1177/1461348419875351
journals.sagepub.com/home/lfn
 SAGE

Shun-Qi Zhang¹ , Xiao-Yu Zhang², Hong-Li Ji³,
Shen-Shun Ying⁴ and Rüdiger Schmidt⁵

Abstract

Vibrations are usually caused by continuous disturbances with large amplitudes. Different from other control methods, disturbance rejection control is a potential method, which considers the unknown disturbances in the control design. To remedy the shortcomings of the existing disturbance rejection control in the vibration reduction of structures especially under high-frequency periodic disturbances, this paper aims to improve the control ability of the current disturbance rejection control for the vibration suppression of smart structures under any unknown periodic disturbances with high-order frequency or random disturbances varying fast. Afterwards, the refined disturbance rejection control is compared with the previously designed disturbance rejection control with proportional–integral observer and disturbance rejection control with generalized proportional–integral observer on both theoretical and numerical levels.

Keywords

Disturbance rejection control, smart structures, vibration suppression, piezoelectric

Introduction

Composite laminated thin-walled structures are widely used in aerospace and automotive engineering owing to their lightweight and relatively high stiffness. However, these kinds of structures have very high sensitivity for vibrations and very low damping ratios. In order to improve the structural performance, composite structures are proposed to be integrated with piezoelectric materials forming smart structures. Because of the sensory and actuation properties, smart structures have great potential in the applications of vibration control, acoustic control, health monitoring, and energy harvesting.

In the area of vibration or acoustic control, the structural performance strongly depends on the control strategy. Therefore, a mathematical model of smart structures for control design is needed, in order to avoid high expenses for experiments. Among the linear modeling techniques for electro-mechanically coupled smart structures, there exist many approaches using solid elements^{1–3} or plate/shell elements based on various hypotheses, e.g. classical plate hypothesis,^{4–6} first-order shear deformation (FOSD) hypothesis,^{7–10} higher-order shear

¹School of Mechatronic Engineering and Automation, Shanghai University, Shanghai, P.R. China

²School of Mechanical Engineering, Northwestern Polytechnical University, Xi'an, P.R. China

³State Key Laboratory of Mechanics and Control of Mechanical Structures, Nanjing University of Aeronautics and Astronautics, Nanjing, P.R. China

⁴Ministry of Education Key Laboratory of Special Purpose Equipment and Advanced Processing Technology, Zhejiang University of Technology, Hangzhou, P.R. China

⁵Institute of Structural Mechanics and Lightweight Design, RWTH Aachen University, Aachen, Germany

Corresponding author:

Shen-Shun Ying, Ministry of Education Key Laboratory of Special Purpose Equipment and Advanced Processing Technology, Zhejiang University of Technology, Hangzhou 310023, P.R. China.

Email: yss@zjut.edu.cn



deformation hypothesis,^{11–13} and zigzag hypothesis.^{14–16} Additionally, for nonlinear modeling, many researchers developed geometrically nonlinear models, e.g. Mukherjee and Chaudhuri,¹⁷ Lentzen et al.,¹⁸ Dash and Singh,¹⁹ Zhang and Schmidt,²⁰ and Zhang et al.²¹ among others, and a few developed electro-elastic materially nonlinear models.^{22,23}

A good vibration suppression ability needs a proper and well-designed control strategy. Based on the mathematical model of smart structures, many control schemes have been applied and developed for vibration suppression. The most frequently used control strategies are e.g. negative velocity/displacement feedback control,^{7,13,24,25} Lyapunov feedback control,^{24,26,27} bang-bang control,^{28,29} and linear quadratic regulator (LQR)/ linear quadratic Gaussian (LQG) control.^{16,30,31} Furthermore, many other advanced control schemes were developed for smart structures, for example independent modal space control,^{32,33} model predictive control,³⁴ sliding mode control,^{35,36} and robust control.^{37–39} Furthermore, without using a mathematical model, some intelligent control methods can be applied, like neural network control^{40–44} and fuzzy logic-based control.^{45–47}

All the control strategies mentioned above only took the displacement or velocity as the measured output, and fed them back to controllers. They did not take into account the disturbances in the control design, due to the difficulty or impossibility of the measurement for unknown disturbances. However, most of the vibrations or acoustics are caused by disturbances, which have relatively large amplitudes compared to noises. In order to provide an effective control for vibration reduction, disturbances might be estimated using an observer, and afterwards the estimated signals are fed back to the controller. Concerning observation systems, several papers developed various observers for the estimation of unknown disturbances or other variables, for example, Hou and Müller,⁴⁸ and Darouach et al.^{48,49} developed full- and reduced-order observers, Söffker et al.,⁵⁰ Morales and Alvarez-Ramirez,⁵¹ König and Mammari,⁵² and Müller⁵³ developed proportional–integral (PI) observers, and Kalsi et al.⁵⁴ and Zhu⁵⁵ developed sliding-mode observers.

Based on the estimated signal, the disturbances can be compensated by a control scheme, here called disturbance rejection (DR) control. The very early development of DR control with PI observer (DR-PI) can be found in the literature.^{56,57} Later, the method was applied to various nonlinear problems by Müller⁵⁸ and Söffker and Müller.^{50,53} Due to limitations of PI observers, the DR-PI control can only estimate and compensate unknown disturbances, which have low frequency or vary slowly. To break through the weakness of PI observers, a generalized proportional–integral (GPI) observer was proposed and developed recently by Zhang et al.^{9,59} The corresponding DR control with GPI observer (DR-GPI) has excellent performance in estimation and compensation of periodic disturbances with both higher and lower order frequency, in case the frequency is roughly or exactly known. Additionally, the disturbance position and the impact factor should be known in both the DR-PI and DR-GPI control schemes.

The literature survey reveals that the existing DR control strategies have very excellent control ability in some aspect, but they are still weak in applications to structures under periodic disturbances with high frequency. This paper aims to improve the current DR control, such that the refined DR control possesses very good ability in the vibration suppression for smart structures under any unknown periodic disturbances with high frequency or random disturbances varying fast. After that, the refined DR control as well as the DR-PI and DR-GPI control are theoretically analyzed and numerically compared.

Dynamic model of smart structures

With regard to smart structures comprising plates or shells, a two-dimensional FE method can be applied based on the Reissner–Mindlin hypothesis. By using Hamilton's principle, a linear dynamic FE model can be obtained as

$$\mathbf{M}_{uu}\ddot{\mathbf{q}} + \mathbf{C}_{uu}\dot{\mathbf{q}} + \mathbf{K}_{uu}\mathbf{q} + \mathbf{K}_{u\phi}\phi_a = \mathbf{F}_{ue} \quad (1)$$

$$\mathbf{K}_{\phi u}\mathbf{q} + \mathbf{K}_{\phi\phi}\phi_s = 0 \quad (2)$$

Here, \mathbf{M}_{uu} , \mathbf{C}_{uu} , \mathbf{K}_{uu} , $\mathbf{K}_{u\phi}$, $\mathbf{K}_{\phi u}$, $\mathbf{K}_{\phi\phi}$ denote the mass matrix, the damping matrix, the stiffness matrix, the piezoelectric coupling matrix, the coupled capacity matrix, and the piezoelectric capacity matrix, respectively. Furthermore, \mathbf{F}_{ue} , \mathbf{q} , ϕ_a , and ϕ_s are respectively the external force vector, the nodal displacement vector, the actuation voltage vector, and the sensor voltage vector. The overhead one dot and two dots denote respectively

the first and the second time derivatives. For more derivation details of the system matrices, please refer to our previous publication.^{9,59}

For the convenience of control design, a state-space model should be derived based on the dynamic FE model. We assume the state variable \mathbf{x} , control input \mathbf{u} , system output \mathbf{y} , and disturbance input \mathbf{f} as

$$\mathbf{x} = \begin{bmatrix} \mathbf{q} \\ \dot{\mathbf{q}} \end{bmatrix}, \quad \mathbf{u} = \phi_a, \quad \mathbf{y} = \phi_s, \quad \mathbf{f} = \mathbf{F}_{ue} \quad (3)$$

A state-space model can be constructed as

$$\dot{\mathbf{x}}(t) = \mathbf{A}\mathbf{x}(t) + \mathbf{B}\mathbf{u}(t) + \mathbf{N}\mathbf{f}(t) \quad (4)$$

$$\mathbf{y}(t) = \mathbf{C}\mathbf{x}(t) \quad (5)$$

$$\mathbf{z}(t) = \mathbf{F}\mathbf{x}(t) + \mathbf{G}\mathbf{u}(t) \quad (6)$$

where the system matrices \mathbf{A} , the control matrix \mathbf{B} , the disturbance influence matrix \mathbf{N} , and the output matrix \mathbf{C} are

$$\mathbf{A} = \begin{bmatrix} \mathbf{0} & \mathbf{I} \\ -\mathbf{M}_{uu}^{-1}\mathbf{K}_{uu} & -\mathbf{M}_{uu}^{-1}\mathbf{C}_{uu} \end{bmatrix}, \quad \mathbf{B} = \begin{bmatrix} \mathbf{0} \\ -\mathbf{M}_{uu}^{-1}\mathbf{K}_{u\phi} \end{bmatrix}, \quad \mathbf{N} = \begin{bmatrix} \mathbf{0} \\ \tilde{\mathbf{M}}_{uu}^{-1} \end{bmatrix}, \quad \mathbf{C} = \begin{bmatrix} -\mathbf{K}_{\phi\phi}^{-1}\mathbf{K}_{\phi u} & 0 \end{bmatrix} \quad (7)$$

The state-space model in equations (4) to (6) has a disturbance input term $\mathbf{N}\mathbf{f}$, which is slightly different from that used in conventional control design. Moreover, the disturbance influence matrix \mathbf{N} should be known. The disturbance vector \mathbf{f} can include any type of input, like external forces in this model, which have relatively large amplitudes compared to noises. In most of the cases, vibrations are caused by disturbances.

Conventional disturbance rejection control

Observation models

Disturbances applied to smart structures are usually unknown and can be of various types. Further assuming that the unknown disturbance vector is composed of a linear part and a residual error part, it leads to

$$\mathbf{f}(t) = \mathbf{H}\mathbf{v}(t) + \Delta(t) \quad (8)$$

where \mathbf{H} is a coefficient matrix, $\mathbf{v}(t)$ denotes a vector of base functions, and $\Delta(t)$ represents a residual error vector, which can be neglected. Taking the derivative of the base functions yields a state-space form of a fictitious disturbance model

$$\mathbf{f}(t) \approx \mathbf{H}\mathbf{v}(t) \quad (9)$$

$$\dot{\mathbf{v}}(t) = \mathbf{V}\mathbf{v}(t) \quad (10)$$

Here, \mathbf{H} and \mathbf{V} denote the coefficient matrices respectively for the output and system matrices of the fictitious model.

Due to various types of disturbances, the components of the disturbance vector can be expressed by many forms of expressions, like Fourier series or high-order polynomial functions.⁹ In the simulation part, periodic disturbances are mainly considered. Therefore, the components of the disturbance vector are assumed to be expressed by finite terms of Fourier series

$$f_i \approx a_{i0} \quad (11)$$

$$\text{or } f_i \approx a_{i0} + a_{i1} \cos(\omega_{i1} t) \quad (12)$$

The resulting coefficient matrices \mathbf{H} and \mathbf{V} associated with equation (11) lead to the proportional–integral (PI) observer⁵³

$$\mathbf{H} = \mathbf{I}, \quad \mathbf{V} = 0 \quad (13)$$

While the coefficient matrices associated with equation (12) lead to the generalized proportional–integral (GPI) observer^{9,59}

$$\mathbf{H} = \begin{bmatrix} 1 & 1 & 0 \end{bmatrix}, \quad \mathbf{V} = \begin{bmatrix} 0 & 0 & 0 \\ 0 & 0 & -\omega_a \\ 0 & \omega_a & 0 \end{bmatrix} \quad (14)$$

where ω_a is the assumed disturbance frequency, determined by the designer.

Closed-loop models

In the framework of DR control, the estimated disturbances are fed back to the controller like the estimated state variables. Therefore, the control law can be defined as

$$\mathbf{u}(t) = -\mathbf{K}_x \hat{\mathbf{x}}(t) - \mathbf{K}_v \hat{\mathbf{v}}(t) \quad (15)$$

where the control gain \mathbf{K}_x is obtained through LQR method, and \mathbf{K}_v can be solved by specific means, with the details in literature.⁵⁹ Further substituting equation (15) into the state-space model (4)–(6), one obtains the closed-loop system as

$$\begin{bmatrix} \dot{\mathbf{x}} \\ \dot{\mathbf{e}}_x \\ \dot{\hat{\mathbf{v}}} \end{bmatrix} = \begin{bmatrix} \mathbf{A} - \mathbf{BK}_x & \mathbf{BK}_x & -\mathbf{BK}_v \\ 0 & \mathbf{A} - \mathbf{L}_x \mathbf{C} & -\mathbf{NH} \\ 0 & \mathbf{L}_v \mathbf{C} & \mathbf{V} \end{bmatrix} \begin{bmatrix} \mathbf{x} \\ \mathbf{e}_x \\ \hat{\mathbf{v}} \end{bmatrix} + \begin{bmatrix} \mathbf{N} \\ \mathbf{N} \\ 0 \end{bmatrix} \mathbf{f} \quad (16)$$

$$\mathbf{y} = \begin{bmatrix} \mathbf{C} & 0 & 0 \end{bmatrix} \begin{bmatrix} \mathbf{x} \\ \mathbf{e}_x \\ \hat{\mathbf{v}} \end{bmatrix} \quad (17)$$

In the conventional DR control, the disturbance influence matrix \mathbf{N} must be known, as it appears in the system matrix of the closed-loop system, which means that the impact factor and the position of the applied disturbances should be known. However, the disturbance itself can be unknown. As mentioned before, the coefficient matrices of the PI observer are receptively identity and zero matrices. DR control with PI observer has an excellent ability on the vibration suppression of smart structures under unknown disturbances with low frequency. For disturbances with higher order frequency, DR-PI control will fail to suppress vibrations, due to low dynamic performance of the observer system. This weak point was improved by Zhang et al.,⁵⁹ in which the PI observer was extended to GPI observer. Because of unknown parameters existing in matrix \mathbf{V} of the GPI observer, a good control effect can be obtained if the assumed frequency ω_a is close to the actual one ω_d of the real disturbance, with the best result when $\omega_a = \omega_d$.

Generalized disturbance rejection control

Refined state-space model

In the conventional DR control, the disturbance influence matrix should be known. Moreover, for higher order frequency disturbances, DR-PI control fails, and DR-GPI control works well but it needs to know the disturbance

frequency. To remedy the aforementioned shortcomings, firstly a refined state-space model is proposed, such that the closed-loop system does not contain the disturbance influence matrix N .

Based on the plant state space model given in equations (4) to (5), introducing a new state variable

$$z = \begin{bmatrix} y \\ \dot{y} \end{bmatrix} \quad (18)$$

a refined state-space model can be derived as

$$\dot{z} = \tilde{A}z + \tilde{B}u + \tilde{N}\tilde{f} \quad (19)$$

$$y = \tilde{C}z \quad (20)$$

Here, the refined system matrix, control matrix, output matrix, and disturbance influence matrix are respectively

$$\tilde{A} = \begin{bmatrix} 0 & I \\ 0 & 0 \end{bmatrix}, \quad \tilde{B} = \begin{bmatrix} 0 \\ CAB \end{bmatrix}, \quad \tilde{C} = [I \ 0], \quad \tilde{N} = \begin{bmatrix} I \\ 0 \end{bmatrix} \quad (21)$$

The new disturbance \tilde{f} is constructed as

$$\tilde{f} = CA(Ax + Nf) + CB\dot{u} + CN\dot{f} \quad (22)$$

From the matrix arrangement of B, C, N , it can be easily seen that $CB = CN = 0$, which yields

$$\tilde{f} = CA(Ax + Nf) \quad (23)$$

Here, the new disturbance includes the actual disturbance, as well as the plant state variables, which is defined as generalized disturbance. The resulting DR control based on the refined state-space model is called the generalized disturbance rejection (GDR) control.

Proportional–integral observer design

Following the design procedure of conventional PI observer, the generalized disturbance is assumed to be composed of a linear and a residual error part as

$$\tilde{f}(t) = H\nu(t) + \Delta(t) \quad (24)$$

Neglecting the residual error and using step function to represent the generalized disturbance, the fictious model can be derived as

$$\tilde{f} = H\nu \quad (25)$$

$$\dot{\nu} = V\nu \quad (26)$$

where $H = I$ and $V = 0$.

The extended model for the refined state-space model can be derived by introducing a new state variable comprised of z and ν as

$$\begin{bmatrix} \dot{z} \\ \dot{\nu} \end{bmatrix} = \begin{bmatrix} \tilde{A} & \tilde{N}H \\ 0 & V \end{bmatrix} \begin{bmatrix} z \\ \nu \end{bmatrix} + \begin{bmatrix} \tilde{B} \\ 0 \end{bmatrix} u \quad (27)$$

$$\mathbf{y} = [\tilde{\mathbf{C}} \quad 0] \begin{bmatrix} \mathbf{z} \\ \mathbf{v} \end{bmatrix} \quad (28)$$

Here, the system matrix and the output matrix of the extended system are defined as

$$\mathbf{A}_e = \begin{bmatrix} \tilde{\mathbf{A}} & \tilde{\mathbf{N}}\mathbf{H} \\ 0 & \mathbf{V} \end{bmatrix}, \quad \mathbf{C}_e = [\tilde{\mathbf{C}} \quad 0] \quad (29)$$

The extended observer system can be constructed as

$$\begin{bmatrix} \dot{\hat{\mathbf{z}}} \\ \dot{\hat{\mathbf{v}}} \end{bmatrix} = \mathbf{A}_b \begin{bmatrix} \hat{\mathbf{z}} \\ \hat{\mathbf{v}} \end{bmatrix} + \begin{bmatrix} \tilde{\mathbf{B}} \\ 0 \end{bmatrix} \mathbf{u} + \begin{bmatrix} \mathbf{L}_z \\ \mathbf{L}_v \end{bmatrix} \mathbf{y} \quad (30)$$

where

$$\mathbf{A}_b = \begin{bmatrix} \tilde{\mathbf{A}} - \mathbf{L}_z \tilde{\mathbf{C}} & \tilde{\mathbf{N}}\mathbf{H} \\ -\mathbf{L}_v \tilde{\mathbf{C}} & \mathbf{V} \end{bmatrix} \quad (31)$$

Observer gain design

The observer gains must be well designed to stabilize the observation system. There are many ways to determine the observer gains \mathbf{L}_z and \mathbf{L}_v , e.g. Lyapunov method, Riccati approach, and pole placement method. The first two methods for DR control were well described in literature.⁵⁹

Riccati approach. The observer gains are assumed as

$$\begin{bmatrix} \mathbf{L}_x^T & \mathbf{L}_v^T \end{bmatrix} = \mathbf{C}_e \mathbf{P}^{-1} \quad (32)$$

where the positive definite matrix \mathbf{P} can be solved by the following standard Riccati equation

$$\mathbf{A}_e \mathbf{P}^{-1} + \mathbf{P}^{-1} \mathbf{A}_e^T - 2\mathbf{P}^{-1} \mathbf{C}_e^T \mathbf{C}_e \mathbf{P}^{-1} + b\mathbf{I} = 0 \quad (33)$$

Here, b is a parameter for observer design, larger b produces larger observer gains.

Pole placement method. The aim of the observer design is to let the observation system stable, meaning that all the eigenvalues of \mathbf{A}_b must be placed in the left half-plane. Rearranging the observation system matrix, one obtains

$$\mathbf{A}_b = \begin{bmatrix} -\mathbf{L}_{z1} & \mathbf{I} & 0 \\ -\mathbf{L}_{z2} & 0 & \mathbf{I} \\ -\mathbf{L}_v & 0 & 0 \end{bmatrix} \quad (34)$$

The eigenvalues can be derived by solving the following characteristic polynomial function of \mathbf{A}_b

$$\begin{aligned} |s\mathbf{I} - \mathbf{A}_b| &= \begin{vmatrix} s\mathbf{I} + \mathbf{L}_{z1} & -\mathbf{I} & 0 \\ \mathbf{L}_{z2} & s\mathbf{I} & -\mathbf{I} \\ \mathbf{L}_v & 0 & s\mathbf{I} \end{vmatrix} \\ &= |s^3\mathbf{I} + s^2\mathbf{L}_{z1} + s\mathbf{L}_{z2} + \mathbf{L}_v| = 0 \end{aligned} \quad (35)$$

Further assume that the observer gains, \mathbf{L}_{z1} , \mathbf{L}_{z2} , and \mathbf{L}_v , are diagonal matrices. The corresponding components of observer gains are respectively l_{1i} , l_{2i} , and l_{3i} , such that the characteristic polynomial function can be

arranged as

$$|s\mathbf{I} - \mathbf{A}_b| = \prod_{i=1}^m (s^3 + l_{1i}s^2 + l_{2i}s + l_{3i}) = \prod_{i=1}^m \left(s + \frac{1}{T_{oi}}\right)^3 = 0 \quad (36)$$

where T_{oi} is a parameter proportional to the settling time. Therefore, all the poles of \mathbf{A}_b will be placed in the left half-plane if T_{oi} satisfies

$$T_{oi} > 0, \quad (i = 1, 2, \dots, m) \quad (37)$$

Usually, smaller T_{oi} leads to a more robust observer system.

Closed-loop control system

Due to the framework of disturbance rejection control, the control input is modified to

$$\mathbf{u} = -\mathbf{K}_z \mathbf{z} - \mathbf{K}_v \hat{\mathbf{v}} \quad (38)$$

Here, the state variable is measurable and used directly, which is the typical difference compared with the conventional DR control. Usually the state variables are unknown in the conventional DR control, the estimated state variables are used in a feedback loop. The control gain for the dynamic part \mathbf{K}_z is obtained by the LQR optimization method, while that for generalized disturbance is solved by specific manner, as can be found in literature.⁵³

Assuming a new state variable for the closed-loop system as

$$\tilde{\mathbf{x}} = [\mathbf{x} \quad \mathbf{z} \quad \mathbf{e}_z \quad \hat{\mathbf{v}}]^T \quad (39)$$

with $\mathbf{e}_z = \mathbf{z} - \hat{\mathbf{z}}$, one obtains the closed-loop system as

$$\begin{bmatrix} \dot{\mathbf{x}} \\ \dot{\mathbf{z}} \\ \dot{\mathbf{e}}_z \\ \dot{\hat{\mathbf{v}}} \end{bmatrix} = \begin{bmatrix} \mathbf{A} & -\mathbf{BK}_z & 0 & -\mathbf{BK}_v \\ \tilde{\mathbf{N}}\mathbf{C}\mathbf{A}\mathbf{A} & \tilde{\mathbf{A}} - \tilde{\mathbf{B}}\mathbf{K}_z & 0 & -\tilde{\mathbf{B}}\mathbf{K}_v \\ \tilde{\mathbf{N}}\mathbf{C}\mathbf{A}\mathbf{A} & 0 & \tilde{\mathbf{A}} - \mathbf{L}_z\tilde{\mathbf{C}} & \tilde{\mathbf{N}}\mathbf{H} \\ 0 & 0 & \mathbf{L}_v\tilde{\mathbf{C}} & \mathbf{V} \end{bmatrix} \begin{bmatrix} \mathbf{x} \\ \mathbf{z} \\ \mathbf{e}_z \\ \hat{\mathbf{v}} \end{bmatrix} + \begin{bmatrix} \mathbf{N} \\ \tilde{\mathbf{N}}\mathbf{C}\mathbf{A}\mathbf{N} \\ \tilde{\mathbf{N}}\mathbf{C}\mathbf{A}\mathbf{N} \\ 0 \end{bmatrix} \mathbf{f} \quad (40)$$

$$\mathbf{y} = \begin{bmatrix} 0 & \tilde{\mathbf{C}} & 0 & 0 \end{bmatrix} \begin{bmatrix} \mathbf{x} \\ \mathbf{z} \\ \mathbf{e}_z \\ \hat{\mathbf{v}} \end{bmatrix} \quad (41)$$

Additionally, the control input can be reconstructed as

$$\mathbf{u} = \begin{bmatrix} 0 & -\mathbf{K}_z & 0 & -\mathbf{K}_v \end{bmatrix} \begin{bmatrix} \mathbf{x} \\ \mathbf{z} \\ \mathbf{e}_z \\ \hat{\mathbf{v}} \end{bmatrix} \quad (42)$$

Here, the GDR control with PI observer is denoted as the GDR-PI control.

Active control simulation

Description of piezoelectric plate structure

A cantilevered composite plate structure bonded with two piezoelectric layers at the upper and lower surfaces, proposed by Lam et al.,⁴ is shown in Figure 1. The host structure in the middle is made of T300/976

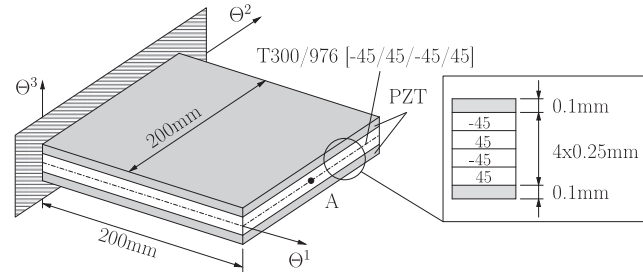


Figure 1. A cantilevered plate with piezoelectric layers.

Table 1. Material properties of the smart plate.

T300/976	PZT
$Y_1 = 150 \text{ GPa}$	$Y = 63 \text{ GPa}$
$Y_2 = 9 \text{ GPa}$	$\nu = 0.3$
$G_{12} = G_{13} = 7.1 \text{ GPa}$	$\rho = 7600 \text{ kg/m}^3$
$G_{23} = 2.5 \text{ GPa}$	$d_{31} = d_{32} = -2.54 \times 10^{-10} \text{ C/N}$
$\nu = 0.3$	$\epsilon_{33} = 1.5 \times 10^{-8} \text{ F/m}$
$\rho = 1600 \text{ kg/m}^3$	

Table 2. First six eigenfrequencies of the plate.

Modes	Present	Lam et al. ⁴	Deviation (%)
1	21.5083	21.4655	0.1994
2	63.2409	63.3468	0.1672
3	129.9076	130.8108	0.6904
4	183.4276	182.4012	0.5627
5	217.8606	218.2537	0.1801
6	382.1172	381.9080	0.0548

graphite–epoxy composite materials with four uniform thickness substrate layers sequenced as $[-45^\circ/45^\circ/-45^\circ/45^\circ]$. The thickness of each composite substrate layer and PZT layer are respectively 0.25 mm and 0.1 mm. The material properties of T300/976 and PZT are listed in Table 1.

The upper layer of PZT is acting as a sensor, while the lower one is an actuator. An unknown disturbance is applied on tip point A. The dynamic FE model is derived by a discretization of 5×5 elements with uniformly reduced integration over the elements. Moreover, the damping matrix is assumed as Rayleigh damping coefficient with the ratio of 0.8% for the first six modes. For validation test, the first six eigenfrequencies are calculated, as shown in Table 2, and compared with those in literature,⁴ which shows very excellent agreement.

Parameter configuration

In the control simulation, three control methods are implemented into vibration suppression of smart structures, namely LQR control, DR control with PI observer (DR-PI), DR control with GPI observer (DR-GPI), GDR control with PI observer (GDR-PI). The control parameters for the control strategies are listed in Table 3. From the parameter configuration in the table, it can be clearly recognized that the frequency of periodic disturbance should be known in DR-GPI control, which is not necessary for other controllers.

To analyze the performance of the GDR-PI control, various groups of parameters with changing \bar{R} or T_o are considered, as listed in Table 4. Two groups of parameters, LQR and GDR-PI, are selected from Table 3 for reference. Decreasing each \bar{R} by 100 times yields parameters for GDR-PI-1 ~3. Alternatively, decreasing each T_o by 10 times leads to parameters for GDR-PI-4 ~6.

Table 3. Parameters for various control strategies.

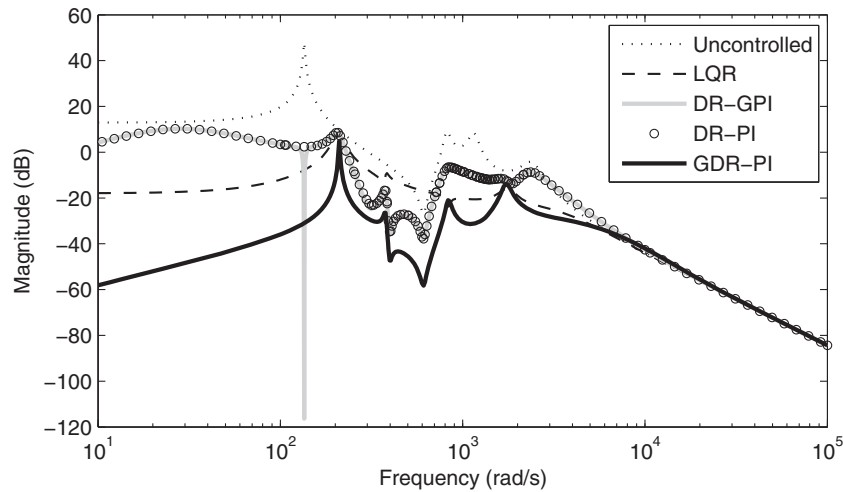
Control method	Common parameters	Other parameters	Observer solution
LQR	$\bar{Q} = 10^{-2}, \bar{R} = 10^{-6}$	None	None
DR-PI	$\bar{Q} = 10^{-2}, \bar{R} = 10^{-6}$	$b = 10^5$	ARE
DR-GPI	$\bar{Q} = 10^{-2}, \bar{R} = 10^{-6}$	$b = 10^5, \omega_a = \omega_d$	ARE
GDR-PI	$\bar{Q} = 10^{-2}, \bar{R} = 10^{-6}$	$T_o = 10^{-4}$	PPM

LQR: linear quadratic regulator; DR-PI: disturbance rejection control with proportional–integral; DR-GPI: disturbance rejection with generalized proportional–integral; GDR-PI: generalized disturbance rejection with proportional–integral; ARE: algebraic Riccati equation; PPM: pole placement method.

Table 4. Parameters for study of the GDR-PI control.

Control method	Common parameters	Other parameters	Observer solution
LQR	$\bar{Q} = 10^{-2}, \bar{R} = 10^{-6}$	None	None
GDR-PI	$\bar{Q} = 10^{-2}, \bar{R} = 10^{-6}$	$T_o = 10^{-4}$	PPM
GDR-PI-1	$\bar{Q} = 10^{-2}, \bar{R} = 10^{-8}$	$T_o = 10^{-4}$	PPM
GDR-PI-2	$\bar{Q} = 10^{-2}, \bar{R} = 10^{-10}$	$T_o = 10^{-4}$	PPM
GDR-PI-3	$\bar{Q} = 10^{-2}, \bar{R} = 10^{-12}$	$T_o = 10^{-4}$	PPM
GDR-PI-4	$\bar{Q} = 10^{-2}, \bar{R} = 10^{-6}$	$T_o = 10^{-5}$	PPM
GDR-PI-5	$\bar{Q} = 10^{-2}, \bar{R} = 10^{-6}$	$T_o = 10^{-6}$	PPM
GDR-PI-6	$\bar{Q} = 10^{-2}, \bar{R} = 10^{-6}$	$T_o = 10^{-7}$	PPM

LQR: linear quadratic regulator; GDR-PI: generalized disturbance rejection with proportional–integral; PPM: pole placement method.

**Figure 2.** Bode plot of the smart plate.

Amplitude–frequency response characteristics

Based on the parameters given in Table 3, the frequency response of the uncontrolled system, the closed-loop system of LQR, DR-PI, DR-GPI, and GDR-PI control can be presented by a Bode plot, as shown in Figure 2. The parameter table shows that the common parameters for all control schemes are the same, and the latter three schemes have additional parameters. As discussed in literature,^{9,59} the parameter b is used to stabilize the observer system, which has very slight influence on the frequency response if it is large enough. Note that the parameter T_o of GDR-PI significantly affects the frequency response. Generally, the smaller T_o , the better the characteristics of the frequency response.

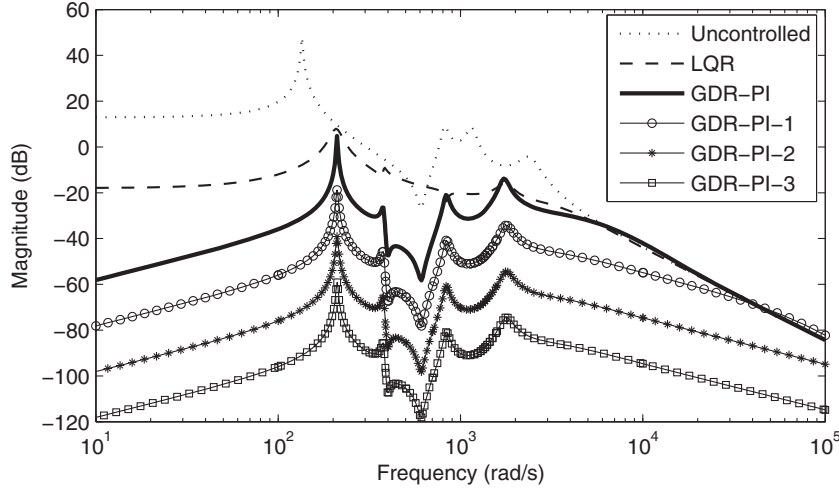


Figure 3. Frequency analysis of GDR-PI with changing T_o .

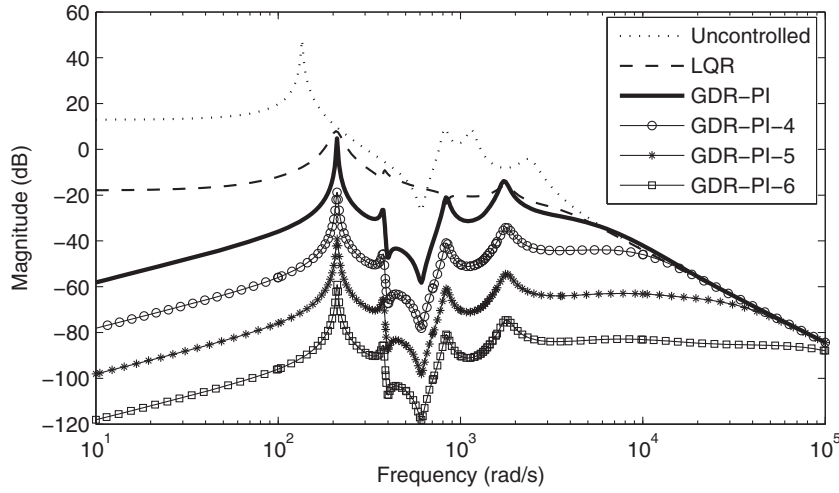


Figure 4. Frequency analysis of GDR-PI with changing \bar{R} .

From Figure 2, it can be seen that the controlled systems (LQR, DR-PI, DR-GPI, GDR-PI) have lower amplitudes than the uncontrolled system. Because LQR is an ideal control scheme, all state variables are fed back to the controller, which is not possible in a real system. In DR-PI and DR-GPI, the estimated state variables are used in the closed-loop system. That is the reason why LQR has smaller amplitudes than DR-PI and DR-GPI control, especially in the lower range of frequency. However, for DR-GPI control, since the frequency of disturbance is assumed to be known, it leads to significant lower amplitudes around the assumed frequency. In GDR-PI control, the mathematical model is absolutely different from conventional DR models. Therefore, it can reach extremely lower amplitudes by setting T_o or (\bar{Q}, \bar{R}) .

To deeply understand the GDR-PI control, several groups of parameters are considered in the following simulations. Decreasing each T_o by 10 times, the frequency-amplitude characteristics change greatly, as shown in Figure 3. The smaller T_o generates smaller amplitudes of vibrations. Alternatively, keeping T_o constant and decreasing each \bar{R} by 100 times, one obtains the frequency plot, as shown in Figure 4. A similar tendency can be obtained, that is smaller \bar{R} produces smaller amplitudes of vibrations.

Time response analysis of vibration suppression

Considering a periodic disturbance waving at the first eigenfrequency of the structure, $f = 0.1\cos(135.1387t)$ N, applied at point A, the time response can be obtained as shown in Figure 5. The figure generally shows that the

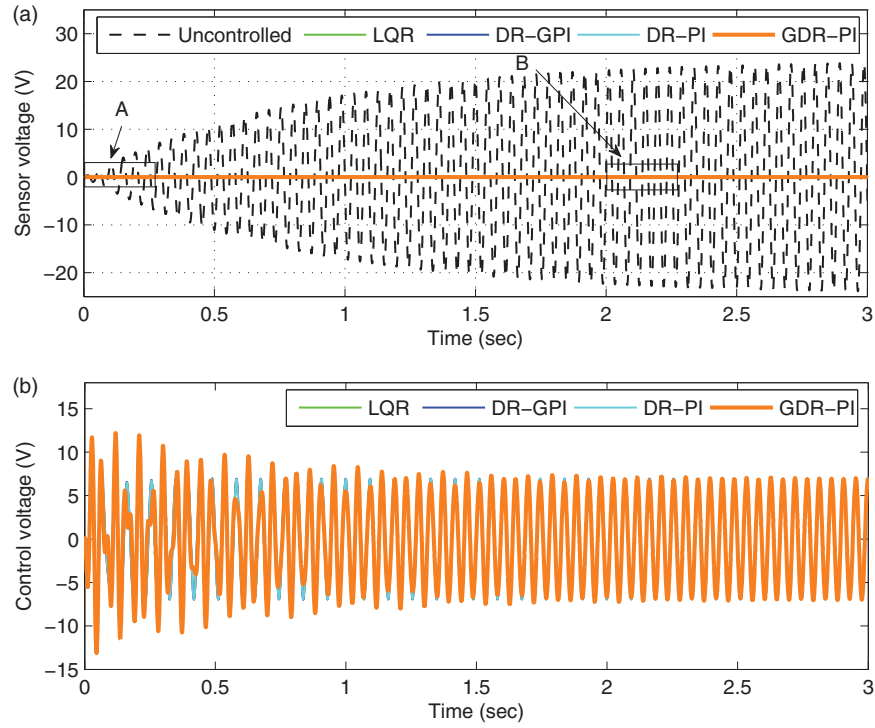


Figure 5. The dynamic behavior of the smart plate under a harmonic disturbance force with the frequency $\omega_d = 21.508$ Hz: (a) sensor output and (b) control input.

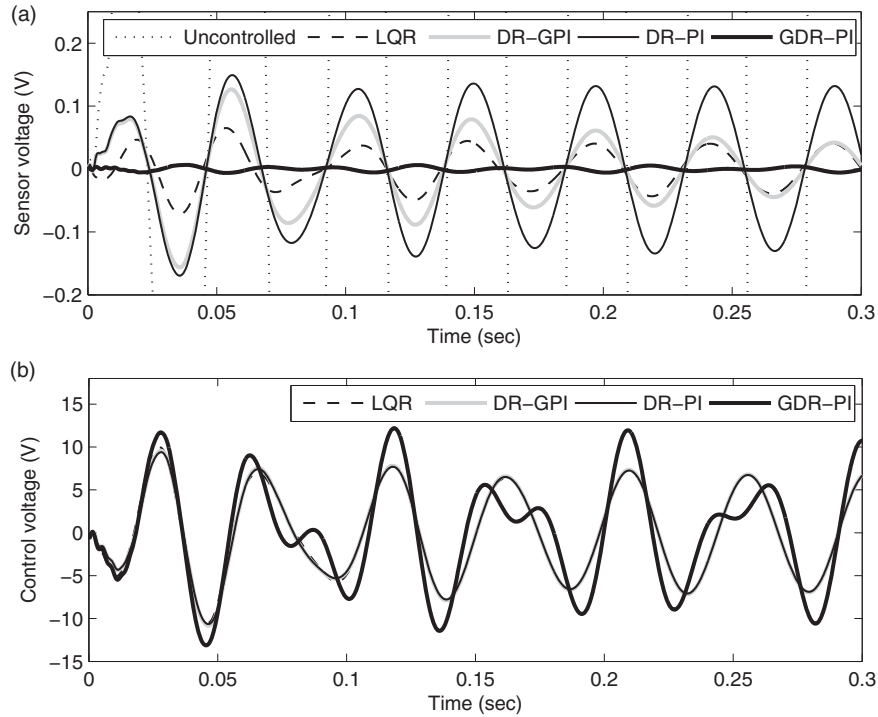


Figure 6. The dynamic behavior of the smart plate under a harmonic disturbance force with the frequency $\omega_d = 21.508$ Hz, section A: (a) sensor output and (b) control input.

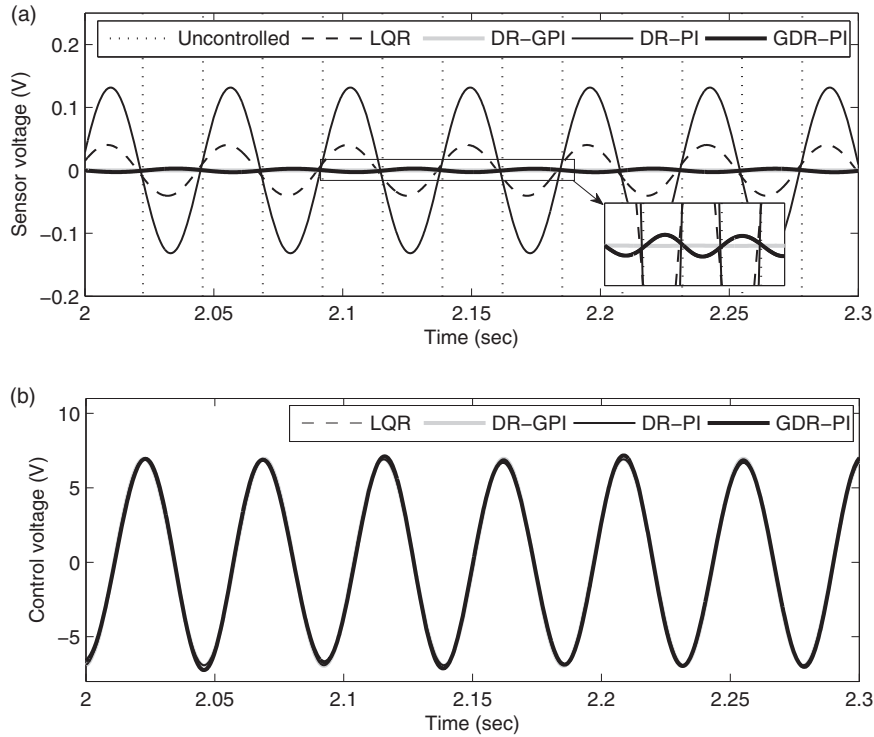


Figure 7. The dynamic behavior of the smart plate under a harmonic disturbance force with the frequency $\omega_d = 21.508$ Hz, section B: (a) sensor output and (b) control input.

controlled systems have significant ability in vibration suppression. Going into section A and B, the details will be clearly shown in Figures 6 and 7.

In the first stage, from 0 s to 0.3 s, it shows that GDR-PI performs best in vibration suppression in comparison with others. Due to the fact that the DR-PI control strategy fails to estimate the disturbance with relatively high frequency (first eigenfrequency), it leads to negative effect on vibration control, and only the free vibration is counteracted. Therefore, the DR-PI control cannot be better than the LQG control, and should be worse than the LQR control. Compared with the DR-PI control, a much better control result can be obtained by the DR-GPI control with increase of time. This is because the DR-GPI control can estimate the disturbance very precisely even with higher order frequency. However, the GPI observer needs rising time to follow the real disturbance. This is the reason that at the very beginning the result of DR-GPI is very close to that of DR-PI, and later the former one gets smaller amplitudes of vibration with increasing time. Going into the details of section B given in Figure 7, time from 2 s to 2.3 s, the results of DR-GPI shows excellent performance, since the GPI observer predicts the disturbance perfectly in the stable state.

Conclusions

Based on the conventional DR control, this paper has developed a GDR control with PI observer, for the vibration suppression of smart structures especially in the range of higher order frequency. In comparison to conventional DR control methods, DR-PI control and DR-GPI control, the current GDR-PI possesses very excellent performance.

From the simulation results, it can be seen that the parameters of (\bar{Q}, \bar{R}) and T_o significantly influence the amplitude–frequency characteristic plots. For the vibration suppression of structures under high-order periodic frequency, GDR-PI performs best when compared with LQR, DR-PI, and DR-GPI in the first beginning period. After the system gets stable, the amplitudes of vibration suppressed by DR-GPI control become the smallest ones. The reason being that the GPI observer contains the frequency information of the real disturbance. However, the GPI needs rising time to follow exactly the real disturbance. This is why the control effect of DR-GPI is worse than that of GDR-PI in the first starting stage.

Declaration of conflicting interests

The author(s) declared no potential conflicts of interest with respect to the research, authorship, and/or publication of this article.

Funding

The author(s) disclosed receipt of the following financial support for the research, authorship, and/or publication of this article: This work was partially supported by the National Natural Science Foundation of China (Grant No. 11972020 and 11602193), the Opening Fund of the State Key Laboratory of Mechanics and Control of Mechanical Structures, Nanjing University of Aeronautics and Astronautics, China (Grant No. MCMS-0517G01), the Nature Science Foundation of Shaanxi Province (Grant No. 2017JQ1027), and the Opening Fund of the State Key Laboratory of Structural Analysis for Industrial Equipment, Dalian University of Technology, China (Grant No. GZ1709).

ORCID iD

Shun-Qi Zhang  <https://orcid.org/0000-0003-0633-0564>

References

1. Kapuria S and Dube GP. Exact piezothermoelastic solution for simply supported laminated flat panel in cylindrical bending. *Z Angew Math Mech* 1997; 77: 281–293.
2. Ray MC, Bhattacharya R and Samanta B. Exact solutions for dynamic analysis of composite plates with distributed piezoelectric layers. *Comput Struct* 1998; 66: 737–743.
3. Sze KY and Yao LQ. A hybrid stress ANS solid-shell element and its generalization for smart structure modeling: part I, solid shell element formulation. *Int J Numer Method Eng* 2000; 48: 545–564.
4. Lam KY, Peng XQ, Liu GR, et al. A finite-element model for piezoelectric composite laminates. *Smart Mater Struct* 1997; 6: 583–591.
5. Kioua H and Mirza S. Piezoelectric induced bending and twisting of laminated composite shallow shells. *Smart Mater Struct* 2000; 9: 476–484.
6. Moita JMS, Correia IFP, Soares CM, et al. Active control of adaptive laminated structures with bonded piezoelectric sensors and actuators. *Comput Struct* 2004; 82: 1349–1358.
7. Wang SY, Quek ST and Ang KK. Vibration control of smart piezoelectric composite plates. *Smart Mater Struct* 2001; 10: 637–644.
8. Krommer M. Piezoelastic vibrations of composite Reissner-Mindlin-type plates. *J Sound Vib* 2003; 263: 871–891.
9. Zhang SQ, Li HN, Schmidt R, et al. Disturbance rejection control for vibration suppression of piezoelectric laminated thin-walled structures. *J Sound Vib* 2014; 333: 1209–1223.
10. Zhang SQ, Li YX and Schmidt R. Modeling and simulation of macro-fiber composite layered smart structures. *Compos Struct* 2015; 126: 89–100.
11. Correia VMF, Gomes MAA, Suleman A, et al. Modelling and design of adaptive composite structures. *Comput Method Appl Mech Eng* 2000; 185: 325–346.
12. Correia IFP, Soares CMM, Soares CAM, et al. Active control of axisymmetric shells with piezoelectric layers: a mixed laminated theory with a high order displacement field. *Comput Struct* 2002; 80: 2265–2275.
13. Moita JS, Martins PG, Soares CMM, et al. Optimal dynamic control of laminated adaptive structures using a higher order model and a genetic algorithm. *Comput Struct* 2008; 86: 198–206.
14. Kapuria S. An efficient coupled theory for multilayered beams with embedded piezoelectric sensory and active layers. *Int J Solids Struct* 2001; 38: 9179–9199.
15. Kapuria S, Dumir PC and Ahmed A. An efficient coupled layerwise theory for dynamic analysis of piezoelectric composite beams. *J Sound Vib* 2003; 261: 927–944.
16. Vasques CMA and Rodrigues JD. Active vibration control of smart piezoelectric beams: comparison of classical and optimal feedback control strategies. *Comput Struct* 2006; 84: 1402–1414.
17. Mukherjee A and Chaudhuri AS. Nonlinear dynamic response of piezolaminated smart beams. *Comput Struct* 2005; 83: 1298–1304.
18. Lentzen S, Klosowski P and Schmidt R. Geometrically nonlinear finite element simulation of smart piezolaminated plates and shells. *Smart Mater Struct* 2007; 16: 2265–2274.
19. Dash P and Singh BN. Nonlinear free vibration of piezoelectric laminated composite plate. *Finite Elem Anal Des* 2009; 45: 686–694.
20. Zhang S and Schmidt R. Static and dynamic FE analysis of piezoelectric integrated thin-walled composite structures with large rotations. *Compos Struct* 2014; 112: 345–357.
21. Zhang SQ, Wang ZX, Qin XS, et al. Geometrically nonlinear analysis of composite laminated structures with multiple macro-fiber composite (MFC) actuators. *Compos Struct* 2016; 150: 62–72.

22. Yao LQ, Zhang JG, Lu L, et al. Nonlinear extension and bending of piezoelectric laminated plate under large applied field actuation. *Smart Mater Struct* 2004; 13: 404–414.
23. Zhang SQ, Zhao GZ, Zhang SY, et al. Geometrically nonlinear FE analysis of piezoelectric laminated composite structures under strong driving electric field. *Compos Struct* 2017; 181: 112–120.
24. Balamurugan V and Narayanan S. Shell finite element for smart piezoelectric composite plate/shell structures and its application to the study of active vibration control. *Finite Elem Anal Des* 2001; 37: 713–738.
25. Kang YK, Park HC, Kim J, et al. Interaction of active and passive vibration control of laminated composite beams with piezoelectric sensors/actuators. *Mater Des* 2002; 23: 277–286.
26. Tzou HS and Tseng CI. Distributed structural identification and control of shells using distributed piezoelectric: theory and finite element analysis. *Dyn Control* 1991; 1: 297–320.
27. Narayanan S and Balamurugan V. Finite element modeling of piezolaminated smart structures for active vibration control with distributed sensors and actuators. *J Sound Vib* 2003; 262: 529–562.
28. Tzou HS and Chai WK. Design and testing of a hybrid polymeric electrostrictive/piezoelectric beam with bang-bang control. *Mech Syst Signal Process* 2007; 21: 417–429.
29. Zhang HY and Shen YP. Vibration suppression of laminated plates with 1-3 piezoelectric fiber-reinforced composite layers equipped with integrated electrodes. *Compos Struct* 2007; 79: 220–228.
30. Dong XJ, Meng G and Peng JC. Vibration control of piezoelectric smart structures based on system identification technique: numerical simulation and experimental study. *J Sound Vib* 2006; 297: 680–693.
31. Li FM and Song ZG. Flutter and thermal buckling control for composite laminated panels in supersonic flow. *J Sound Vib* 2013; 332: 5678–5695.
32. Chen CQ and Shen YP. Optimal control of active structures with piezoelectric modal sensors and actuators. *Smart Mater Struct* 1997; 6: 403–409.
33. Lin JC and Nien MH. Adaptive control of a composite cantilever beam with piezoelectric damping-modal actuators/sensors. *Compos Struct* 2005; 70: 170–176.
34. Dubay R, Hassan M, Li C, et al. Finite element based model predictive control for active vibration suppression of a one-link flexible manipulator. *ISA Trans* 2014; 53: 1609–1619.
35. Manjunath TC and Bandyopadhyay B. Vibration control of Timoshenko smart structures using multirate output feedback based discrete sliding mode control for SISO systems. *J Sound Vib* 2009; 326: 50–74.
36. Lin CY and Jheng HW. Active vibration suppression of a motor-driven piezoelectric smart structure using adaptive fuzzy sliding mode control and repetitive control. *Appl Sci* 2017; 7: 240.
37. Hu YR and Vukovich G. Active robust shape control of flexible structures. *Mechatronics* 2005; 15: 807–820.
38. Marinova DG, Stavroulakis GE and Zacharenakis C. Robust control of smart beams in the presence of damage-induced structural uncertainties. In: *Proceedings of international conference on physics and control*, 2005, pp. 339–344.
39. Hasheminejad SM, Vahedi M and Markazi AHD. Multi-objective robust active vibration control of an arbitrary thick piezolaminated beam. *Mech Compos Mater Struct* 2015; 22: 908–924.
40. Valoor MT, Chandrashekhara K and Agarwal S. Self-adaptive vibration control of smart composite beams using recurrent neural architecture. *Int J Solids Struct* 2001; 38: 7857–7874.
41. Jha R and He C. Neural and conventional adaptive predictive controllers for smart structures. In: *44th AIAA/ASME/ASCE/AHS structures, structural dynamics, and materials conference*, No. AIAA 2003-1808. Norfolk, VA: American Institute of Aeronautics and Astronautics, Inc., 2003.
42. Kumar R, Singh SP and Chandrawat HN. MIMO adaptive vibration control of smart structures with quickly varying parameters: neural networks vs classical control approach. *J Sound Vib* 2007; 307: 639–661.
43. Qiu Z, Zhang X and Ye C. Vibration suppression of a flexible piezoelectric beam using BP neural network control. *Acta Mech Solid Sin* 2012; 25: 417–428.
44. Abdeljaber O, Avci O and Inman D. Active vibration control of flexible cantilever plates using piezoelectric materials and artificial neural networks. *J Sound Vib* 2016; 363: 33–53.
45. Abreu GL and Ribeiro JF. A self-organizing fuzzy logic controller for the active control of flexible structures using piezoelectric actuators. *Appl Soft Comput* 2002; 1: 271–283.
46. Shirazi AHN, Owji HR and Rafeeyan M. Active vibration control of an FGM rectangular plate using fuzzy logic controllers. *Procedia Eng* 2011; 14: 3019–3026.
47. Marinaki M, Marinakis Y and Stavroulakis GE. Fuzzy control optimized by a multi-objective differential evolution algorithm for vibration suppression of smart structures. *Comput Struct* 2015; 147: 126–137.
48. Hou M and Müller PC. Design of observers for linear systems with unknown inputs. *IEEE Trans Autom Control* 1992; 37: 871–875.
49. Darouach M, Zasadzinski M and Xu SJ. Full-order observers for linear systems with unknown inputs. *IEEE Trans Autom Control* 1994; 39: 606–609.
50. Söffker D, Yu TJ and Müller PC. State estimation of dynamical systems with nonlinearities by using proportional-integral observer. *Int J Syst Sci* 1995; 26: 1571–1582.
51. Morales A and Alvarez-Ramirez J. A PI observer for a class of nonlinear oscillators. *Phys Lett A* 2002; 297: 205–209.

52. Koenig D and Mammar S. Design of proportional-integral observer for unknown input descriptor systems. *IEEE Trans Autom Control* 2002; 47: 2057–2062.
53. Müller PC. Design of PI-observers and -compensators for nonlinear control systems. In: Chernousko FL, Kostin GV and Saurin VV (eds) *Proceedings of the 14th international workshop on dynamics and control*, Moscow-Zvenigorod, Russia, 2007, pp. 223–231.
54. Kalsi K, Lian J, Hui S, et al. Sliding-mode observers for systems with unknown inputs: a high-gain approach. *Automatica* 2010; 46: 347–353.
55. Zhu F. State estimation and unknown input reconstruction via both reduced-order and high-order sliding mode observers. *J Process Control* 2012; 22: 296–302.
56. Müller PC and Lückel J. Optimal multivariable feedback system design with disturbance rejection. *Prob Control Inform Theory* 1977; 6: 211–227.
57. Müller PC and Lückel J. Zu der Störgrößenaufschaltung in linearen Mehrgrößenregelsystemen. *Regelungstechnik* 1977; 25: 54–59.
58. Müller PC. Indirect measurement of nonlinear effects by state observer. In: W Schiehlen (ed.) *IUTAM symposium on nonlinear dynamics in engineering system*. Berlin: Springer-Verlag, 1990, pp. 205–215.
59. Zhang SQ, Schmidt R, Müller PC, et al. Disturbance rejection control for vibration suppression of smart beams and plates under a high frequency excitation. *J Sound Vib* 2015; 353: 19–37.